"Rainbow" Trapping and Releasing at Telecommunication Wavelengths

Qiaoqiang Gan,* Yujie J. Ding, and Filbert J. Bartoli†

Center for Optical Technologies, Electrical and Computer Engineering Department, Lehigh University, Bethlehem, Pennsylvania 18015, USA

(Received 11 July 2008; revised manuscript received 31 December 2008; published 2 February 2009)

The reported "trapped rainbow" storage of THz light in metamaterials and plasmonic graded structures has opened an attractive new method to control electromagnetic radiation. Here, we show how, by incorporating the frequency-dependent dielectric properties of the metal, the graded grating structures developed for "trapped rainbow" storage of THz light in μm level can be scaled to nm level for telecommunication waves for applications in optical communication and various nanophotonic circuits.

DOI: 10.1103/PhysRevLett.102.056801 PACS numbers: 73.20.Mf, 42.25.Bs, 42.79.Gn, 78.68.+m

It was demonstrated previously that very cold gases [1] may be used to slow down electromagnetic (EM) radiation. In recent years, researchers made several breakthroughs of employing photonic crystals to slow down EM radiation in both theory [2–5] and experiment [6–9], such as stopping light all optically [5], actively controlling slow light [6], indirectly or directly observing the guided modes for slow light [7], trapping and delaying photons in a nanocavity [8], and exploiting low-dispersion or even dispersionless properties using gap solitons [9]. While promising steps have been taken towards slowing down light in solid-state media including semiconductor nanostructures operating at room temperature [10], "stopping" light completely and implementation in optoelectronic devices [11] on a chip remain a great challenge. Recent reports on "trapped rainbow" storage of THz light in metamaterials [2] and plasmonic graded structures [3] have opened a new and attractive approach to stopping light. It was shown that tapered waveguides with a negative refractive index core [2] or graded metallic grating structures [3,4] were capable of slowing light to a standstill at different locations. The advantages of these schemes are the ability to reduce the speed of the light over a wide range of wavelengths and temperatures, including room temperature [3]. Since that plasmonic structures and devices operating in the optical domain offer significant advantages for merging photonics and electronics within nanoscale dimensions [12], it is of value to incorporate the dispersion properties of the metal and scale the operating frequencies of these structures from THz to telecommunication domain, or even to visible domain to trap a rainbow visible to humans.

Scaling laws [13] indicate how the cutoff frequency in the dispersion relations of periodic gratings can be easily scaled to other frequency regimes. In this work, we explore decreasing the feature sizes of metal gratings (see the inset in Fig. 1) to nanoscale dimensions to extend operational frequencies to the visible and infrared domains, and examine the dispersion properties of the metal nanostructures in detail. We employ the complex refractive indices of the metal, in this case silver [14] (see Fig. S1 in the supplementary material [15]), and determine the dispersion relations of the gratings by means of the finite-difference-time-domain (FDTD) simulations [16]. As can be shown by the results in Fig. 1, the cutoff frequencies of the silver gratings with structure 1 ($h = 230$ nm, $d = 200$ nm, $p = 400$ nm) and structure 2 ($h = 140$ nm, $d = 200$ nm, $p = 400$ nm) are now both in the telecommunication domain [1.7808×10^{14} Hz ($\lambda = 1.6846$ μm) for structure 1 and $2.266\,37 \times 10^{14}$ Hz ($\lambda = 1.3237$ μm) for structure 2, respectively].

It is known that the group velocity, v_g, of surface-plasmon-polariton (SPP) modes, which is given by the slope of the tangent line at a given point on the dispersion curve, decreases significantly with increasing the frequency as the cutoff frequency is approached [3,4]. Consequently, if the light at the cutoff frequency is coupled into the grating structure, its v_g becomes quite low. However, it remains a considerable challenge to overcome the large momentum mismatch in the first Brillouin zone and to directly couple the light into one of the SPP modes

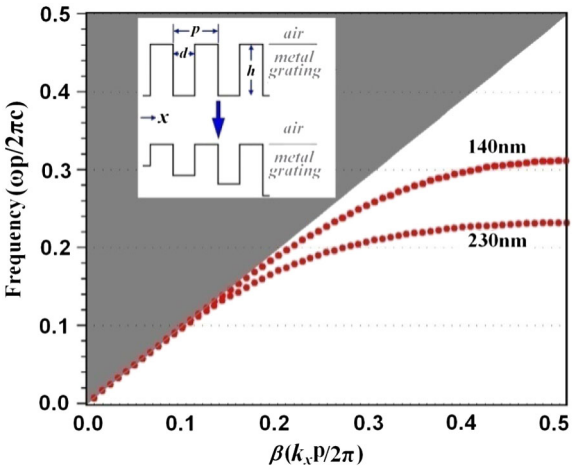

FIG. 1 (color online). Dispersion curves calculated for $d = 200$ nm and $p = 400$ nm with different groove depths ($h = 140$ and 230 nm). Inset: a schematic of grating structures with a constant depth and graded depth. In this figure, the x axis is the reduced propagation constant with a unit of $k_x p/2\pi$; the y axis is the reduced frequency with a unit of $\omega p/2\pi c$, here c is the light velocity in vacuum.

around the cutoff frequency. In a recent study, the v_g of SPP modes at telecommunication frequencies was reported to be approximately half that of the light velocity [17], which implies that the working frequency is still far away from the cutoff frequency.

To address the issues of optical coupling and momentum mismatch, we employ the graded grating structure illustrated in Fig. 1 to gradually couple light into SPP modes possessing a very low v_g. Assuming that the grade is small enough, a graded grating could be approximated by a series of many small gratings, each with a constant groove depth. The dispersion relations for such a nonuniform grating are expected to change gradually along the x axis as the groove depth is increased. If a wave propagates along the surface of such a grating, the v_g of the SPP mode gradually decreases along the propagation direction. By properly choosing the grating depths, the v_g for an incoming wave can be greatly reduced and it can even approach zero at a specific location. For example, let us assume that the groove depth changes gradually from 140 to 230 nm over the 25 μm grating length. For this structure, the dispersion relations will vary as a function of position along the grating, roughly changing from the dispersion curve shown for 140 nm in Fig. 1 to that for 230 nm. At the input port, the shallow end of the grating, we only need to overcome a relatively small momentum mismatch to couple the light into the SPP mode. Subsequently, this mode will couple, step by step, as it enters into regions of increasing grating depth. This series of steps was introduced to help overcome the large momentum mismatch and gradually couple light into SPP modes with a large value of k_x and a very small v_g. It should also be noted that as the grating depth changes, so does the cutoff frequency. Therefore, incoming waves at different frequencies will be ''trapped'' at correspondingly different positions having different depths, corresponding, respectively, to different cutoff frequencies, along the grating, leading to the so-called ''trapped rainbow'' storage of light [2,3].

The concept described above can be validated by two-dimensional FDTD simulations. Figure 2 illustrates how light waves at four different wavelengths in the telecommunication domain, i.e., 1.33 μm, 1.45 μm, 1.55 μm, and 1.65 μm, are trapped at different positions along the graded grating structures. These four wavelengths correspond to the cutoff frequencies associated with the grating depths at these positions. According to Fig. 1, the cutoff frequencies for the gratings with constant depths of 140 and 230 nm are about 226.6 THz (i.e., $\lambda \sim 1.32$ μm) and 178.1 THz ($\lambda \sim 1.68$ μm), respectively. These values are in good agreement with those obtained from the FDTD simulations, see Figs. 2(a) and 2(d): As shown in Fig. 2(a), the 1.33 μm wave is trapped at $x = 13$ μm, where the grating depth is about 150 nm. Similarly Fig. 2(d) shows how the 1.65 μm wave is trapped at about $x = 20.5$ μm, where the grating depth is about 225 nm. By further reducing the feature size of the graded gratings, one should

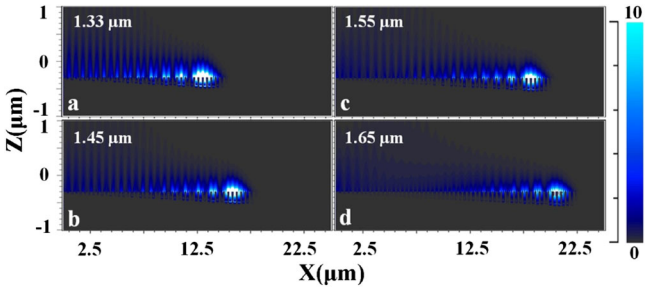

FIG. 2 (color online). Trapped rainbow for telecommunication wavelengths obtained by using two-dimensional FDTD simulations: (a)–(d) correspond to the 2D field distribution at four different wavelengths of 1.33, 1.45, 1.55, and 1.65 μm. The depth of the grating structure changes from 20 to 270 nm linearly in a 25 μm region. In these simulations, the period and width of the grating structure are 400 and 200 nm, respectively. Nonuniform mesh sizes are employed in this modeling: The edge grid sizes are $\Delta x = 10$ nm and $\Delta z = 2$ nm, and body grid sizes are $\Delta x = 20$ nm and $\Delta z = 20$ nm. The simulation time $T = 2000$ μm$/c$, here c is the light velocity in vacuum.

be able to ''trap'' waves in the visible domain (see Fig. S2 in the supplementary material [15]). Interestingly, some recent experimental results based on photonic crystals demonstrated that a photonic-crystal waveguide with a graded hole size is capable of slowing down and trapping light at different wavelengths to different positions within the waveguide [18].

The next question that arises after trapping the telecommunication rainbow at different locations along the graded grating is how to release the trapped waves. One method for releasing these waves is to cap the metal grating with a dielectric material and temperature-tune the refractive index of the material filling the grooves via the thermo-optic effect [19]. In this way, the optical properties of the plasmonic structure can be tuned by changing the refractive index of the material at the interface [12]. For a given temperature change, the thermo-optic effect would produce a much larger change in the dispersion relations than thermal expansion or contraction of metals (the thermal expansion coefficient of silver is, e.g., about 18.9×10^{-6} K^{-1}). For example, the thermo-optic coefficient, dn/dT, of GaAs is about $(2.0 \sim 3.0) \times 10^{-4}$ K^{-1} [19], while its thermal expansion coefficient is only about 5.7×10^{-6} K^{-1}. Consequently, a temperature change of 100 K will increase the refractive index by $0.02 \sim 0.03$ (about 0.6% of the refractive index of 3.37 for GaAs at a wavelength of 1.55 μm [19]). The corresponding change in feature size is only 0.057% and has a negligible effect on the optical properties of the structure. The temperature-dependent refractive index of GaAs is shown by the inset to Fig. 3.

At 200 K, n_{GaAs} is approximately 3.347 and the cutoff frequency for the grating structure ($h = 70$ nm, $d = 200$ nm, $p = 400$ nm) is about 1.927×10^{14} Hz ($\lambda = 1.557$ μm) (see Fig. 3). Surface modes at this frequency

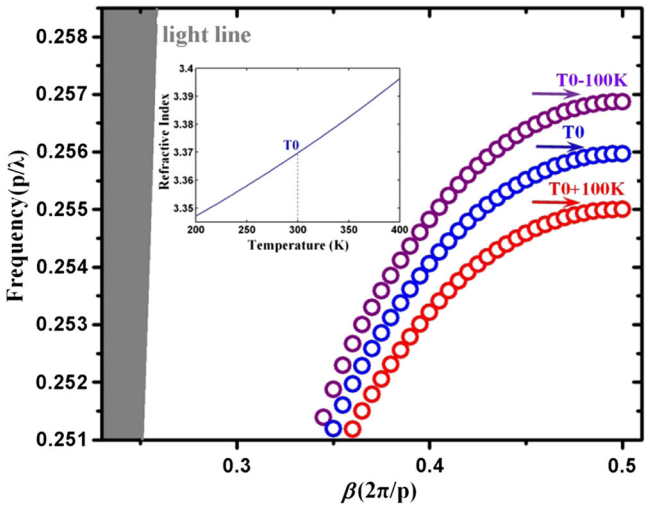

FIG. 3 (color online). Dispersion curves calculated for $d = 200$ nm, $p = 400$ nm and $h = 70$ nm with different temperatures. Inset: the temperature dependence of the refractive index of GaAs around 1.55 μm wavelength. Its thermo-optical coefficient is calculated with the fitting equation: $dn/dT = n(b_0 + b_1T + b_2T^2 + b_3T^3 + b_4T^4 + b_5T^5 + b_6T^6)$. For GaAs at 1.53 μm wavelength, $b_0 = -3.059 \times 10^{-5}$, $b_1 = 12.03 \times 10^{-7}$, $b_2 = -6.442 \times 10^{-9}$, $b_3 = 1.820 \times 10^{-11}$, $b_4 = -2.720 \times 10^{-14}$, $b_5 = 2.047 \times 10^{-17}$, $b_6 = -6.086 \times 10E^{-21}$. This equation is valid from 85 to 920 K [19].

are trapped in the structure. If the temperature is increased by 100 K, n_{GaAs} increases to 3.370. Assuming other grating parameters are unchanged due to the small thermal expansion coefficient, the cutoff frequency would shift to 1.920×10^{14} Hz ($\lambda = 1.563$ μm). In other words, the trapped surface mode at 1.927×10^{14} Hz is no longer supported by the grating, and therefore released at this temperature. Similarly, if the temperature is further increased to 400 K, n_{GaAs} increases to 3.396, and the cutoff frequency shifts to 1.913×10^{14} Hz ($\lambda = 1.569$ μm). As a result, the trapped surface mode at 1.927×10^{14} Hz is also "released." In this way, the trapped waves can be released one by one by temperature-tuning the refractive index of the materials that fill the grating grooves, representing a possible way to realize the optical buffers for future on-a-chip optical communications. Employing materials such as InAs, PbS, and PbSe [19], which exhibit a larger thermo-optic effect, it is feasible to achieve wider temperature tunability through an optimized design that incorporates the actual temperature dependence of these materials [20]. Such a thermo-optical coupling mechanism will open a new route towards active control of the speed of surface waves. However, thermal releasing is a relatively slow process. High speed modulation approaches would be required to make such structures useful for practical optical communication applications. The discussion above indicates that waves at near-infrared and visible wavelengths can be slowed down in the graded grating structures. It remains to be seen how completely the waves can be "stopped" [21,22]. According to the perfect electronic conductor (PEC) model commonly employed for terahertz waves, loss may be neglected [3], and the v_g at the cutoff frequency could be very close to zero. However, at telecommunication and visible wavelengths, the strong metal absorption cannot be neglected, and v_g, i.e., the slope of the dispersion curve at the band edge, is not so close to zero. Consequently, when absorption loss is considered, the plasmonic modes cannot be "stopped" completely. However, their group velocity can be significantly reduced. At the band edge shown in Fig. 1, the v_g of the SPP could be slowed down by $10^3 \sim 10^4$, which could be used for implementing practical slow-light applications [22]. Reflection and scattering are both possible loss mechanisms after the surface modes were guided to their corresponding trapped positions.

We next consider the lifetime of the plasmonic modes in the grating structures to explore their usefulness for practical applications. While we do not directly calculate the lifetime of the SPP in these structures, it can be estimated indirectly from the FDTD simulations, using the expression, $\tau = 1/(\alpha v_g)$, where α is the propagation loss coefficient. The v_g, which is obtained from the slope of the dispersion curve, decreases significantly as the frequency increases towards the cutoff frequency of the metal grating. The propagation loss coefficient α, which depends on both internal absorption and scattering losses, can be determined from the two-dimensional field distribution obtained from FDTD simulations. A large α, which may be expected due to strong metal absorption in the near-infrared and visible spectral regions, would be indicative of a shorter photon lifetime.

We first consider an incoming wave of fixed frequency coupling into SPPs on a flat metal/dielectric interface. When the permittivity of the dielectric layer is increased, the cutoff frequency of the dispersion curve decreases. As the SPP cutoff frequency decreases and becomes closer to the frequency of the light wave, the wave is confined more strongly at the interface. This results in an increase in the energy confined at the interface and penetrating into the metal. Consequently, larger metal absorption and shorter SPP lifetime is expected, as illustrated in Fig. 4(a) (details are discussed in the supplementary material [15]).

We next consider SPPs on grating surfaces with a metal-air interface in the visible and near-IR spectral regions. We currently have neither analytical expressions nor sufficient experimental data for v_g or α, but we can still estimate the lifetime of the plasmonic mode by extracting approximate values of v_g and α from the FDTD simulation (see Fig. S3 in the supplementary material [15]). Figure 4(b) shows that the empirically derived surface plasmon lifetime as a function of groove depth, for a wavelength of 1.70 μm, which is quite different from the behavior obtained for flat metal/dielectric interfaces shown in Fig. 4(a). As the SPP is guided along the graded grating surface in the direction of increasing groove depth, its lifetime increases monotonically with groove depth, reaching a value of approxi-

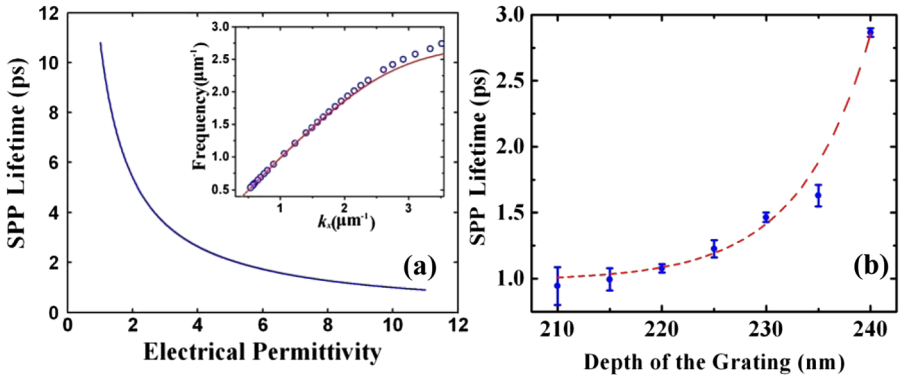

FIG. 4 (color online). (a) Lifetimes of the SPP modes for an incident wavelength of 1.70 μm calculated using Eq. (S4) in [15]. Inset: Dispersion curve for the flat silver/air interface calculated by Eq. (S2) (solid line) [15] and the FDTD method (dots). (b) Estimate of the SPP lifetime, τ, at the wavelength of 1.70 μm along the grating surfaces for various depths. Blue dots are extracted raw data listed in Table S1 [15]. The dashed line is an exponential growth fit to guide the eyes.

mately 3 ps where the groove depth is 240 nm. Such a lifetime may be long enough for some meaningful nanophotonic applications. These estimated lifetimes are of the same order of magnitude as a value reported recently for a somewhat different plasmonic structure [23]. While further investigation is needed, the capability of significantly reducing the v_g of light along the graded grating structures and trapping photons for a long period of time may play a significant role in compact optical-buffer memories, quantum-information/optical processing, and plasmonic active devices.

In summary, we have made feasibility studies on trapping and releasing electromagnetic waves in graded grating structures in the telecommunication and visible domains. Such a phenomenon can be exploited in the novel designs of the plasmonic devices targeted towards the applications in optical buffers, data synchronizers [2], broadband slow-light systems, integrated optical filters [3], wavelength-division multiplexing, on-chip optical interconnectors, spectroscopy, imaging devices [3,12], and nonlinear optical devices.

The authors would like to acknowledge the support of this research by NSF (Grant No. CBET-0608742). Q. G. is indebted to Dr. Thomas L. Koch, Zhan Fu, and Ravi Sekhar Tummidi for helpful discussions.

*qig206@lehigh.edu
†fjb205@lehigh.edu

[1] L. V. Hau, S. E. Harris, Z. Dutton, and C. H. Behroozi, Nature (London) **397**, 594 (1999).
[2] K. L. Tsakmakidis, A. D. Boardman, and O. Hess, Nature (London) **450**, 397 (2007).
[3] Q. Gan, Z. Fu, Y. Ding, and F. Bartoli, Phys. Rev. Lett. **100**, 256803 (2008).
[4] Z. Fu, Q. Gan, Y. Ding, and F. Bartoli, IEEE J. Sel. Top. Quantum Electron. **14**, 486 (2008).
[5] M. F. Yanik and S. H. Fan, Phys. Rev. Lett. **92**, 083901 (2004).
[6] Y. A. Valsov, M. O'Boyle, H. F. Hamann, and S. J. McNab, Nature (London) **438**, 65 (2005).
[7] N. Notomi *et al.*, Phys. Rev. Lett. **87**, 253902 (2001); V. S. Volkov, S. I. Bozhevolnyi, L. H. Frandsen, and M. Kristensen, Nano Lett. **7**, 2341 (2007); H. Gersen *et al.*, Phys. Rev. Lett. **94**, 073903 (2005); R. J. P. Engelen *et al.*, Opt. Express **14**, 1658 (2006).
[8] T. Tanabe *et al.*, Nat. Photon. **1**, 49 (2007).
[9] J. T. Mok, C. Martijn De Sterke, I. C. M. Littler, and B. J. Eggleton, Nature Phys. **2**, 775 (2006).
[10] L. V. Hau, Nat. Photon. **2**, 451 (2008); T. Baba, *ibid.* **2**, 465 (2008); Luc Thevenaz, *ibid.* **2**, 474 (2008).
[11] A. V. Turukhin, V. S. Sudarshanam, M. S. Shahriar, J. A. Musser, B. S. Ham, and P. R. Hemmer, Phys. Rev. Lett. **88**, 023602 (2001); M. S. Bigelow, N. N. Lepeshkin, and R. W. Boyd, *ibid.* **90**, 113903 (2003).
[12] W. L. Barnes, A. Dereux, and T. W. Ebbesen, Nature (London) **424**, 824 (2003); E. Ozbay, Science **311**, 189 (2006); C. Genet and T. W. Ebbesen, Nature (London) **445**, 39 (2007); S. Lal, S. Link, and N. J. Halas, Nat. Photon. **1**, 641 (2007); H. Atwater, Sci. Am. **296**, 56 (2007).
[13] J. D. Joannopoulos, R. D. Meade, and J. N. Winn, *Photonics Crystals: Modeling the Flow of Light* (Princeton University, Princeton, NJ, 1995).
[14] E. D. Palik, *Handbook of Optical Constants of Solids* (Academic, Orlando, FL, 1985), Vol. 1, p. 366.
[15] See EPAPS Document No. E-PRLTAO-102-048907 for the EPAPS supplementary materials. For more information on EPAPS, see http://www.aip.org/pubservs/epaps.html.
[16] Fullwave simulation with the commercial FDTD solver, Fullwave and Bandsolve (Rsoft Inc.), are used to calculate the dispersion relations of the silver grating structures.
[17] M. Sandtke and L. Kuipers, Nat. Photon. **1**, 573 (2007).
[18] R. J. P. Engelen, D. Mori, T. Baba, and L. Kuipers, Phys. Rev. Lett. **101**, 103901 (2008).
[19] Gorachand Ghosh, *Handbook of Thermo-Optic Coefficients of Optical Materials with Applications* (Academic, Orlando, FL, 1998), Vol. 5, p. 234.
[20] J. A. McCaulley, V. M. Donnelly, M. Vernon, and I. Taha, Phys. Rev. B **49**, 7408 (1994).
[21] A. Reza, M. M. Dignam, and S. Hughes, Nature (London) **455**, E10 (2008).
[22] K. L. Tsakmakidis, A. D. Boardman, and O. Hess, Nature (London) **455**, E11 (2008).
[23] A. S. Vengurlekar, A. Venu Gopal, and T. Ishihara, Appl. Phys. Lett. **89**, 181927 (2006).